Jamali, Raha; Bordbar Khiabani, Aydin; Yarmand, Benyamin; Mozafari, Masoud; Kolahi, Alireza

Effects of co-incorporated ternary elements on biocorrosion stability, antibacterial efficacy, and cytotoxicity of plasma electrolytic oxidized titanium for implant dentistry

Published in:
Materials Chemistry and Physics

DOI:
10.1016/j.matchemphys.2021.125436

Published: 15/01/2022

Document Version
Peer-reviewed accepted author manuscript, also known as Final accepted manuscript or Post-print

Please cite the original version:
Jamali, R., Bordbar Khiabani, A., Yarmand, B., Mozafari, M., & Kolahi, A. (2022). Effects of co-incorporated ternary elements on biocorrosion stability, antibacterial efficacy, and cytotoxicity of plasma electrolytic oxidized titanium for implant dentistry. *Materials Chemistry and Physics*, *276*, Article 125436.
https://doi.org/10.1016/j.matchemphys.2021.125436

Effects of co-incorporated ternary elements on biocorrosion stability, antibacterial efficacy, and cytotoxicity of plasma electrolytic oxidized titanium for implant dentistry

Raha Jamali[a], Aidin Bordbar-Khiabani[a,b], Benyamin Yarmand[a,*], Masoud Mozafari[c,d], Alireza Kolahi[a]

[a] Nanotechnology and Advanced Materials Department, Materials and Energy Research Center (MERC), Karaj, Iran

[b] Chemical and Metallurgical Engineering Department, Aalto University, Espoo, Finland

[c] Tissue Engineering and Regenerative Medicine Department, Iran University of Medical Science, Tehran, Iran

[d] Lunenfeld-Tanenbaum Research Institute, Mount Sinai Hospital, University of Toronto, Toronto, Canada

* Corresponding author's email: byarmand@merc.ac.ir

Abstract

In this study, calcium, phosphorus, and copper co-incorporated titanium oxide (TiO_2) layers were prepared on titanium substrates using the plasma electrolytic oxidation process. Thereafter, their features were studied to be used in dental implants. Surface characterization revealed that the addition of calcium and copper ions to the phosphate-based electrolyte led to the development of the ternary elements incorporated TiO_2 layer with greater surface homogeneity, roughness, hydrophobicity, and growth rate. As well, electrochemical impedance spectroscopy proved that the placement of the ternary elements caused more compaction of the TiO_2 layer by reducing inherent defects. Thus, the corrosion behavior of the TiO_2 layer in artificial saliva solution has promoted, which consequently enhanced the corrosion potential by 187 mV and diminished the corrosion current density by one order of magnitude. Antibacterial assessment against *Escherichia coli* showed that incorporation of copper along with calcium and phosphorus significantly restored the bactericidal activity of the TiO_2 layer. Furthermore, the integration, proliferation, and viability of MG-63 osteoblastic cells have considerably improved in the biological response to the calcium, phosphorus, and copper-containing layer.

Keywords: Ternary elements, plasma electrolytic oxidation, biocorrosion, antibacterial activity, cytotoxicity.

1. Introduction

The use of titanium alloys in manufacturing dental implants is limited due to insufficient osseointegration, inadequate corrosion resistance in saliva medium, and bacterial infection [1]. Thus, it is essential to modify the surface features of titanium-based dental implants to achieve the desired characteristics [2]. Plasma electrolytic oxidation (PEO) is a cost-effective, straightforward surface treatment method that can improve the corrosion resistance and cellular response in the biological environment by creating an adhesive rough oxide layer on titanium and its alloys [3]. Accordingly, the main advantage of this process is tailoring the biological properties of the oxide layer by controlling the chemical composition of the electrolyte to attain better functions in the biological medium [3, 4].

Various studies have revealed that the incorporation of calcium via phosphate-based electrolyte would have some beneficial effects on enhancing the bioactivity of PEO-grown layers in the biological environment by inducing osteoconductive compounds [5]. Some reports have also shown that bacterial contamination concomitant with biofilm formation and inflammation of surrounding tissue lead to a high failure rate of dental implants [6]. As one of the most common oral aerobic bacteria, *Escherichia coli* (*E. coli*) has been recognized as the main etiological agent for peri-implantitis [7]. Furthermore, it has been found that copper, as an essential trace element, plays an influential role in bone metabolism through being involved in enzyme-based processes [8]. As well, copper has a bactericidal efficacy, showing superior antibacterial activity and cytotoxicity [9]. The interest in copper-enriched PEO coatings on metallic materials has considerably increased owing to their excellent antibacterial properties and biocompatibility, along with their improved corrosion resistance [10-12]. Recently, Liang et al. [13] fabricated a phosphorous and copper dual elements co-incorporated TiO_2 layer on the surface of Ti-6Al-4V alloy via PEO using EDTA-$CuNa_2$ and phytic acid-containing electrolyte. They demonstrated that phosphorous and copper ions in the electrolyte led to a significant decline in the size of pores and triggered the bone formation upon immersion in a Hank solution for 14 days. They also reported that the PEO-treated surface with larger amounts of incorporated copper could modulate a favorable inflammatory microenvironment for osteoblast-like cell differentiation. However, the corrosion resistance of the prepared coatings has not been studied.

In order to shorten the wound healing time after implantation of the dental implant in the bone tissue, this study aimed to co-dope calcium and phosphorus as the main elements that stimulate bone growth along with copper as an antibacterial agent on the titanium substrate. To the best of our knowledge, there are no studies devoted to the ternary co-incorporation of calcium, phosphorus, and copper elements into the TiO_2 matrix by the PEO method. Moreover, limited studies have been performed on the corrosion behavior of multi-elemental PEO coatings on titanium-based implants in a saliva medium. In this regard, the simultaneous incorporation of the ternary elements was investigated in the oxide layer created by the PEO process. Additionally, their effects on surface properties, corrosion behavior in artificial saliva solution, antibacterial function, and cytotoxicity were precisely characterized.

2. Materials and Methods

2.1. Layer preparation

In the current research, some commercially pure titanium (cp-Ti) plates with dimensions of 20×10×2 mm^3 were treated under a constant current density of 100 $mA.cm^{-2}$ as well as a duty cycle of 50% for 6 min. The phosphate solution including 5 $g.L^{-1}$ Na_3PO_4 (Merck) and 2 $g.L^{-1}$ KOH (Merck) was used as base electrolyte for preparing TiO_2 layer, named as T0. Thereafter, T1 was created by the addition of 1 $g.L^{-1}$ $C_4H_6CaO_4$ (Merck) to the base electrolyte and T2 was then grown by the addition of 2 $g.L^{-1}$ $C_4H_6CuO_4$ (Merck) to the previously-made calcium containing solution.

2.2. Layer characterization

Morphological observations were characterized using field emission scanning electron microscope (FESEM, TESCAN, MIRA III), which was equipped with energy-dispersive X-ray spectroscope (EDS, Oxford INCA). The cross-sectional view of samples was examined by optical microscopy (Zeiss Axioskop2-MAT). The roughness and thickness of the layers were captured using PHYNIX TR-100 and PHYNIX FN testers, respectively. X-ray diffractometer (XRD, Philips PW3710) was also used for phase identification. Notably, wettability was assessed by measuring the contact angle of a 4 μL droplet of deionized water using a digital microscope (Dino-Lit, AM413ZT).

2.3. Electrochemical characterization

Potentiodynamic polarization and electrochemical impedance spectroscopy (EIS) tests were performed in artificial saliva solution at 37 °C using a Potentiostat/Galvanostat (EG & G, 263A) instrument with a three-electrode configuration. A platinum electrode and a saturated Ag/AgCl electrode (SCE) were respectively used as the counter and reference electrodes, and artificial saliva solution was used as the electrolyte. Before performing the measurements, the specimens were left in the open-circuit potential for 1 h to reach stability in artificial saliva solution. The polarization curves were then recorded over a potential range of -1.0 to +1.0 V versus open-circuit potential at a scanning rate of 1 $mV.s^{-1}$. A perturbation potential of 10 mV amplitude was conducted in the frequency range of 10^{-2} to 10^{5} Hz in the EIS test. Finally, EIS analysis and modeling, as well as data extraction, were performed using ZView software.

2.4. Antibacterial assay

Antibacterial activity was evaluated by exposing the sterilized samples using *E. coli* bacterial suspension at a concentration of 1.5×10^{6} $CFU.mL^{-1}$ for 24 h at 37 °C. Thereafter, the antibacterial performance was determined from the percentage of the number of the missed bacterial colonies to the number of the control colonies after 24 h incubation period.

2.5. Cytotoxicity test

Cytotoxicity was assessed by seeding MG-63 osteoblastic cells on the sterilized specimens using Dulbecco's modified Eagle standard medium containing a density of 5×10^{5} $cell.mL^{-1}$ at 37 °C in a humidified 5% CO_2 atmosphere. By passing 24 h from the incubation, cell viability was evaluated using (3-(4,5-dimethylthiazol-2-yl)-2, 5-diphenyltetrazolium bromide (MTT) assay.

2.6. Statistical analysis

The experimental results are expressed as means ± standard deviations. All data were analyzed by Student's *t*-test and one-way analysis of variance (ANOVA). The confidence levels were set as 95% ($p < 0.05$).

3. Results and discussion

The FESEM images of the layers' morphology are illustrated in Figure 1a. All the layers were observed to have a pancake-like microstructure. As well, by the co-incorporation of calcium, phosphorus, and copper (T2), the large pores disappeared and the surface porosity became more homogenous, which indicated better stability of electrical micro-discharges [13]. As a result of the increased distance between the peaks and valleys of the layers' surface, the average surface roughness revealed a rising trend as $R_{T0}=0.45\pm0.08 < R_{T1}=0.53\pm0.05 < R_{T2}=0.68\pm0.02$ µm. As shown in Figure 1b, wettability evaluation revealed that the hydrophobicity of the layers enhanced by the incorporation of ternary ions. The average thickness for samples T0, T1, and T2 was obtained 4.8±0.5, 5.9±0.2, and 6.2±0.5 µm, respectively. The optical microscopic cross-sectional images of samples are shown in Figure S1. As it can be seen, the average thickness values of the T0, T1, and T2 were estimated to be 5.1, 5.8, and 6.4 µm, respectively, which corroborate the data obtained from the modular thickness gauge system. Regarding the EDS spectra in Figure 1c, all the layers were composed of titanium, oxygen, and phosphorus elements. Titanium was related to the substrate, while oxygen was the result of oxidation during the PEO process. The existence of sodium, phosphorus and calcium was attributed to Na_3PO_4 and $C_4H_6CaO_4$ in the electrolyte composition. Moreover, copper was detected in T2 as a result of $C_4H_6CuO_4$. Examining the elemental distribution in T2 by EDS mapping proved that all the added elements of calcium, phosphorus, and copper were incorporated in the structure of the layer and had a uniform distribution similar to titanium and oxygen (Figure 1d). Phase identification demonstrated that anatase and rutile had been formed in all the layers and no crystalline structure containing calcium, phosphorous, or copper was detected (Figure 1e). Obviously, the participation of incorporated ions in electrochemical reactions during the layer growth process led to the predominance of anatase over rutile [14].

Figure 1

The potentiodynamic polarization curves of the layers along with the titanium are displayed in Figure 2a. In addition, by comparing the corrosion characteristics of titanium (i_{corr}= 0.235 μA.cm^{-2}, E_{corr}= -737 mV) with T0 (i_{corr}= 0.182 μA.cm^{-2}, E_{corr}= -294 mV), T1 (i_{corr}= 0.171 μA.cm^{-2}, E_{corr}= -249 mV) and T2 (i_{corr}= 0.095 μA.cm^{-2}, E_{corr}= -107 mV), it was revealed that the oxide layers prevent the degradation of titanium in artificial saliva solution. It was also found that the placement of ternary ions decelerated the kinetics of dissolution reactions and the thermodynamic tendency of the layers against corrosion, in which the protective role of copper was more significant compared to that of calcium and phosphorus [15, 16]. This improvement may be due to the greater thickness of T2 compared to both T0 and T1, which prolong the penetration pathways of aggressive agents through the layer. Furthermore, the useful effects of copper in reducing the chemical affinity of the layers against destruction can be considered as another promoting factor in this regard [17, 18]. For comparison, the i_{corr} values of the metallic ions-incorporated coatings which formed on titanium and its alloys via different surface treatment methods were listed in Table 1. It could be found that the TiO_2 layer produced by the present strategy exhibited the lowest value of i_{corr} when compared to others.

Table 1

Nyquist and Bode's plots resulted from EIS analyses are illustrated in Figure 2b-d. It was observed that T2 has the capacitive loop with the largest diameter. Correspondingly, this specimen also exhibited the highest impedance modulus (~10^6 Ω.cm^2) at low frequencies as well as the highest phase angle (~77°) at high frequencies. The appearance of peak position in high-frequency values suggests the dielectric characteristic of copper on the calcium and phosphorus-containing layer [25]. These results indicate that embedding ternary ions in the layer structure would significantly strengthen its impermeability. The EIS empirical data were modeled using the equivalent circuit inserted in Figure 2b, in which R_s is the series resistance, and $R_{i/o}$ and $CPE_{i/o}$ stand for the resistance and the constant phase element of the inner and outer parts of the layers, respectively [26]. Comparison of the fitted EIS results presented in Table 2 also revealed that the values of $R_{i/o}$ and $CPE_{i/o}$ in both parts of the layers had ascending and descending trends, respectively. So, it can be concluded that the stability of the conditions of the layer formation processes reduced its inherent defects due to the co-participation of ternary ions, and as a result, the diffusion of corrosive ions towards the titanium substrate became more difficult [26, 27].

Figure 2

Table 2

Figure 3a exhibits the optical images of the cultured plates after 24 h incubation period, showing the antibacterial ability of the layers against *E. coli*. The number of bacterial colonies reflects the capability of the sample to inhibit bacterial growth. Figure 3a shows that the number of bacterial colonies on the surface of the PEO coatings is significantly reduced compared with cp-Ti as the coating material inhibits the adhesion and growth of *E. coli*. However, the antibacterial activity of T0 and T2 seems to be higher than T1. Moreover, quantitative analysis of the bactericidal activity of the layers revealed that the antibacterial performances of T0 and T2 are 48% and 58%, respectively. The bactericidal efficacy of T0 may be due to the formation of anatase and rutile, because these compounds can disrupt the integrity of the bacterial cell wall by generating reactive oxygen species [28, 29]. It was shown that the increased affinity for the adsorption of proteins and organic matter to the layer surface due to inducing calcium phosphate compounds in a biological medium can consequently lead to the loss of antibacterial ability in T1 [30]. As well, the incorporation of copper ions into the layer containing calcium ions restored the bactericidal effect due to the positive effect of copper ions on the disintegration of bacterial cytoplasmic membranes and inactivation of metabolic pathways [31]. Furthermore, the enhanced hydrophobicity of the layer is known as another effective factor that may reduce bacterial adhesion [32]. The morphology of MG-63 osteoblastic cells grown on the layers after 24 h incubation period is shown in the FESEM images of Figure 3b. It was discovered that the polygonally matured cells with multiple pseudopodia connections are spreading on the surface of all the layers, indicating the provision of suitable conditions for cell growth and proliferation processes [33]. It was also observed that the extended pseudopodia anchored into the surface pores of the layers and well-conformed, indicating appropriate cell adhesion and integration [34]. Viability assessment of the cultured cells after 24 h of incubation is displayed in Figure 3c, showing that all the layers have excellent cell viabilities and experienced an improving trend due to the placement of ternary ions. This promotion may be due to the morphological changes and the predominance of anatase [35]. Furthermore, the ability of the incorporated copper ions to cross-link collagen to bone elastin may ultimately boost the biological cell response [36].

Figure 3

4. Conclusions

In the present study, calcium, phosphorus, and copper co-incorporated TiO_2 layer were successfully fabricated on titanium by the PEO process. The corrosion measurements in artificial saliva solution signified a corrosion barrier effect for the ternary elements incorporated layer owing to its higher thickness and surface features. Finally, combining calcium, phosphorus, and copper elements on the surface of titanium substrate greatly improves the antibacterial properties and osteoblastic cellular response. Therefore, it will significantly reduce the risk of postoperative bacterial infection and cytotoxicity for implant dentistry.

Acknowledgment

This research work has been supported with research grant (No.: 247383) by Materials and Energy Research Center (MERC), Karaj, Iran.

References

[1] M. Kaur and K. Singh, Review on titanium and titanium based alloys as biomaterials for orthopaedic applications, Materials Science and Engineering: C 102 (2019): 844-862.

[2] D. A. Florea, D. Albuleț, A. M. Grumezescu, E. Andronescu, Surface modification–A step forward to overcome the current challenges in orthopedic industry and to obtain an improved osseointegration and antimicrobial properties, Materials Chemistry and Physics 243 (2020): 122579.

[3] L. L. Rodriguez and P. A. Sundaram, Corrosion behavior of plasma electrolytically oxidized gamma titanium aluminide alloy in simulated body fluid, Materials Chemistry and Physics 181 (2016): 67-77.

[4] T.O.B. Polo, W.P.P. Silva, G.A.C. Momesso, T.J. Lima-Neto, S. Barbosa, et al., Plasma electrolytic oxidation as a feasible surface treatment for biomedical applications: An in vivo study, Scientific Reports 10.1 (2020): 1-11.

[5] A. R. Rafieerad, M. R. Ashra, R. Mahmoodian, A. R. Bushroa, Surface characterization and corrosion behavior of calcium phosphate-base composite layer on titanium and its alloys via plasma electrolytic oxidation: A review paper, Materials Science and Engineering: C 57 (2015): 397-413.

[6] S. Spriano, S. Yamaguchi, F. Baino, S. Ferraris, A critical review of multifunctional titanium surfaces: New frontiers for improving osseointegration and host response, avoiding bacteria contamination, Acta Biomaterialia 79 (2018): 1-22.

[7] O. M. Goudouri, E. Kontonasaki, U. Lohbauer, A. R Boccaccini, Antibacterial properties of metal and metalloid ions in chronic periodontitis and peri-implantitis therapy, Acta Biomaterialia 10.8 (2014): 3795-3810.

[8] M. Zhou, X. Wu, J. Luo, G. Yang, Y. Lu, Copper peptide-incorporated 3D-printed silk-based scaffolds promote vascularized bone regeneration, Chemical Engineering Journal (2021): 130147.

[9] A. Bhattacharjee, S. Das, B. Das, P. Roy, Intercalative DNA binding, protein binding, antibacterial activities and cytotoxicity studies of a mononuclear copper (II) complex, Inorganica Chimica Acta 514 (2021): 119961.

[10] X. Zhang, Y. Wu, J. Wang, X. Xia, Y. Lv et al., Microstructure, formation mechanism and antifouling property of multi-layered Cu-incorporated Al_2O_3 coating fabricated through plasma electrolytic oxidation, Ceramics International 46.3 (2020): 2901-2909.

[11] P. Cerchier, L. Pezzato, E. Moschin, L.B. Coelho, M.G.M. Olivier et al., Antifouling properties of different Plasma Electrolytic Oxidation coatings on 7075 aluminium alloy, International Biodeterioration & Biodegradation 133 (2018): 70-78.

[12] D. Zhang, Q. Han, K. Yu, X. Lu, Y. Liu et al., Antibacterial activities against Porphyromonas gingivalis and biological characteristics of copper-bearing PEO coatings on magnesium, Journal of Materials Science & Technology 61 (2021): 33-45.

[13] T. Liang, Y. Wang, L. Zeng, Y. Liu, L. Qiao, et al., Copper-doped 3D porous coating developed on Ti-6Al-4V alloys and its in vitro long-term antibacterial ability, Applied Surface Science 509 (2020): 144717.

[14] R. Vasilić, S. Stojadinović, N. Radić, P. Stefanov, Z. Dohčević-Mitrović et al. One-step preparation and photocatalytic performance of vanadium doped TiO_2 coatings, Materials Chemistry and Physics 151 (2015): 337-344.

[15] S. Kalaivani, R.K. Singh, V. Ganesan, S. Kannan. Effect of copper (Cu^{2+}) inclusion on the bioactivity and antibacterial behavior of calcium silicate coatings on titanium metal, Journal of Materials Chemistry B 2.7 (2014): 846-858.

[16] Y. Huang, X. Zhang, R. Zhao, H. Mao, Y. Yan, Antibacterial efficacy, corrosion resistance, and cytotoxicity studies of copper-substituted carbonated hydroxyapatite coating on titanium substrate, Journal of Materials Science 50.4 (2015): 1688-1700.

[17] F.S. Da Silva, N. Cinca, S. Dosta, , I.G. Cano, J.M. Guilemany et al., Corrosion resistance and antibacterial properties of copper coating deposited by cold gas spray, Surface and Coatings Technology 361 (2019): 292-301.

[18] X. Xu, L. Zhu, W. Li, H. Liu, A variable hydrophobic surface improves corrosion resistance of electroplating copper coating, Applied Surface Science 257.13 (2011): 5524-5528.

[19] C. Peng, Y. Zhao, S. Jin, J. Wang, R. Liu et al., Antibacterial TiCu/TiCuN multilayer films with good corrosion resistance deposited by axial magnetic field-enhanced arc ion plating, ACS Applied Materials & Interfaces 11.1 (2018): 125-136.

[20] S. Wu, X. Shen, M. Chen, K.H.R. Yie, Z. Zhou et al., Multifunctional TaCu-nanotubes coated titanium for enhanced bacteriostatic, angiogenic and osteogenic properties, Materials Science and Engineering: C 120 (2021): 111777.

[21] I.J. Hwang and H.C. Choe, Effects of Zn and Si ions on the corrosion behaviors of PEO-treated Ti-6Al-4V alloy, Applied Surface Science 477 (2019): 79-90.

[22] X. Zhang, Y. Lv, F. Shan, Y. Wu, X .Lu et al. Microstructure, corrosion resistance, osteogenic activity and antibacterial capability of Mn-incorporated TiO_2 coating, Applied Surface Science 531 (2020): 147399.

[23] P. Manojkumar, E. Lokeshkumar, A. Saikiran, B. Govardhanan, M. Ashok et al., Visible light photocatalytic activity of metal (Mo/V/W) doped porous TiO_2 coating fabricated on Cp-Ti by plasma electrolytic oxidation, Journal of Alloys and Compounds 825 (2020): 154092.

[24] M. Molaei, A. Fattah-Alhosseini, M. K. Keshavarz., Influence of different sodium-based additives on corrosion resistance of PEO coatings on pure Ti, Journal of Asian Ceramic Societies 7.2 (2019): 247-255.

[25] C. Liu, Q. Bi, A. Leyland, A. Matthews, An electrochemical impedance spectroscopy study of the corrosion behaviour of PVD coated steels in 0.5 N NaCl aqueous solution: Part II.: EIS interpretation of corrosion behaviour, Corrosion Science 45.6 (2003): 1257-1273.

[26] A. Bordbar-Khiabani, B. Yarmand, M. Mozafari, Effect of ZnO pore-sealing layer on anti-corrosion and in-vitro bioactivity behavior of plasma electrolytic oxidized AZ91 magnesium alloy, Materials Letters 258 (2020): 126779.

[27] S. Hariprasad, M. Ashfaq, T. Arunnellaiappan, M. Harilal, N. Rameshbabu, Role of electrolyte additives on in-vitro corrosion behavior of DC plasma electrolytic oxidization coatings formed on Cp-Ti, Surface and Coatings Technology 292 (2016): 20-29.

[28] Y. Nosaka, A.Y. Nosaka, Generation and detection of reactive oxygen species in photocatalysis, Chemical Reviews 117.17 (2017): 11302-11336.

[29] S.L. Iconaru, A. Groza, S. Gaiaschi et al., Antimicrobial Properties of Samarium Doped Hydroxyapatite Suspensions and Coatings, Coatings 10.11 (2020): 1124.

[30] M. Kazemzadeh-Narbat, J. Kindrachuk, K. Duan, H. Jenssen, R.E. Hancock et al., Antimicrobial peptides on calcium phosphate-coated titanium for the prevention of implant-associated infections, Biomaterials 31.36 (2010): 9519-9526.

[31] K. Leśniak-Ziółkowska, A. Kazek-Kęsik, K. Rokosz et al., Plasma electrolytic oxidation as an effective tool for production of copper incorporated bacteriostatic coatings on Ti-15Mo alloy, Applied Surface Science (2021): 150284.

[32] G. Wang, D. Weng, C. Chen, L. Chen, J. Wang, Influence of TiO_2 nanostructure size and surface modification on surface wettability and bacterial adhesion, Colloid and Interface Science Communications 34 (2020): 100220.

[33] K. Leśniak-Ziółkowska, A. Kazek-Kęsik, K. Rokosz et al., Electrochemical modification of the Ti-15Mo alloy surface in solutions containing ZnO and $Zn_3(PO_4)_2$ particles, Materials Science and Engineering: C 115 (2020): 111098.

[34] A. Yanovska, Y. Husak, O. Mishchenko, A. Gudakov, O. Oleshko, Cell viability and collagen deposition on hydroxyapatite coatings formed on pretreated substrates, Materials Chemistry and Physics 258 (2021): 123978.

[35] I.J. Hwang, H.C. Choe, Surface morphology and cell behavior of Zn-coated Ti-6Al-4V alloy by RF-sputtering after PEO-treatment, Surface and Coatings Technology 361 (2019): 386-395.

[36] X. Yuan, J. Wang, X. Zhu, Z. Zhang, Y. Ai, Effect of copper on levels of collagen and alkaline phosphatase activity from chondrocytes in newborn piglets in vitro, Biological Trace Element Research 144.1 (2011): 597-605.

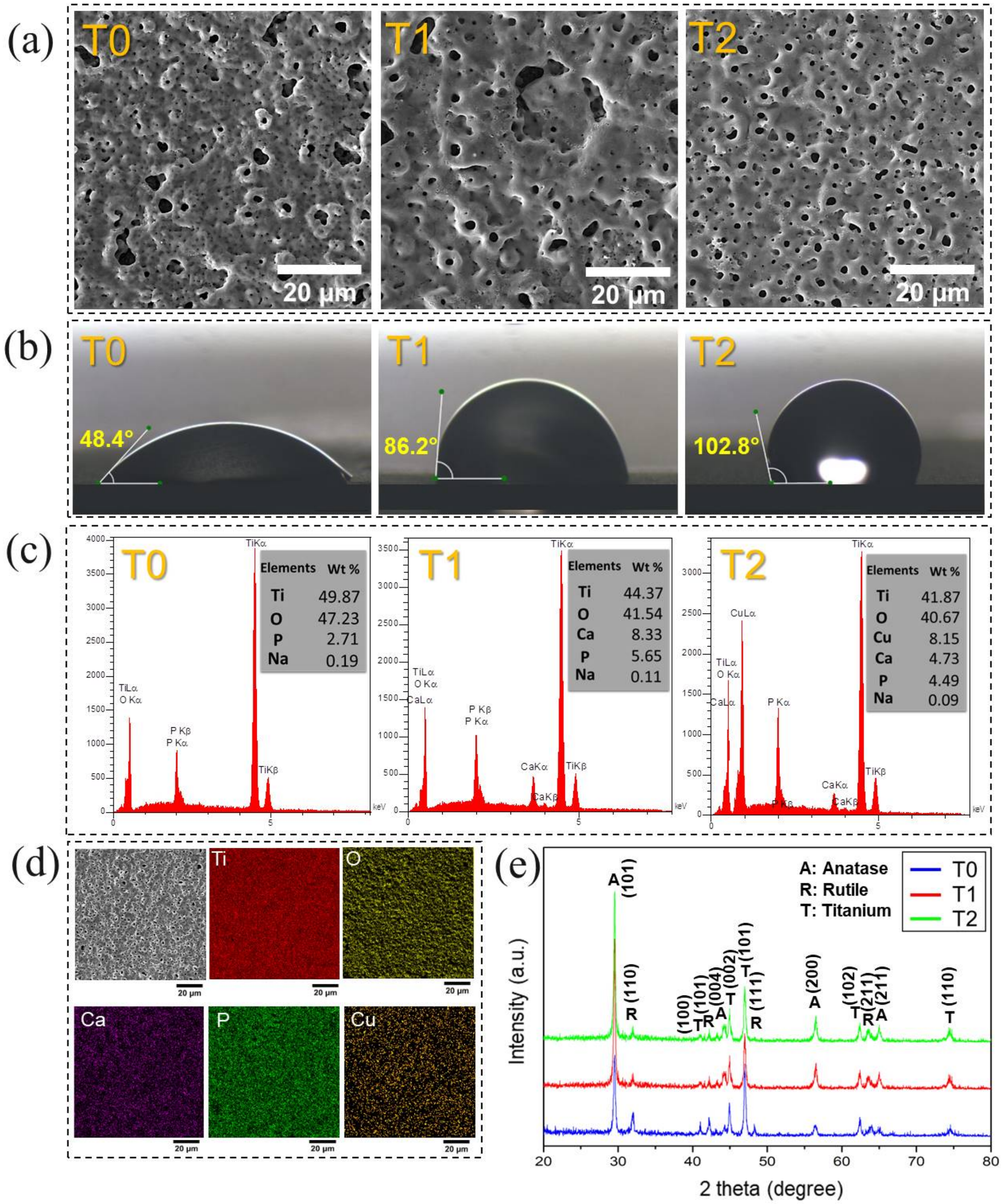

Figure 1. (a) FESEM micrographs, (b) contact angle variations, (c) EDS spectra, (d) EDS maps of T2, and (e) XRD patterns of the layers.

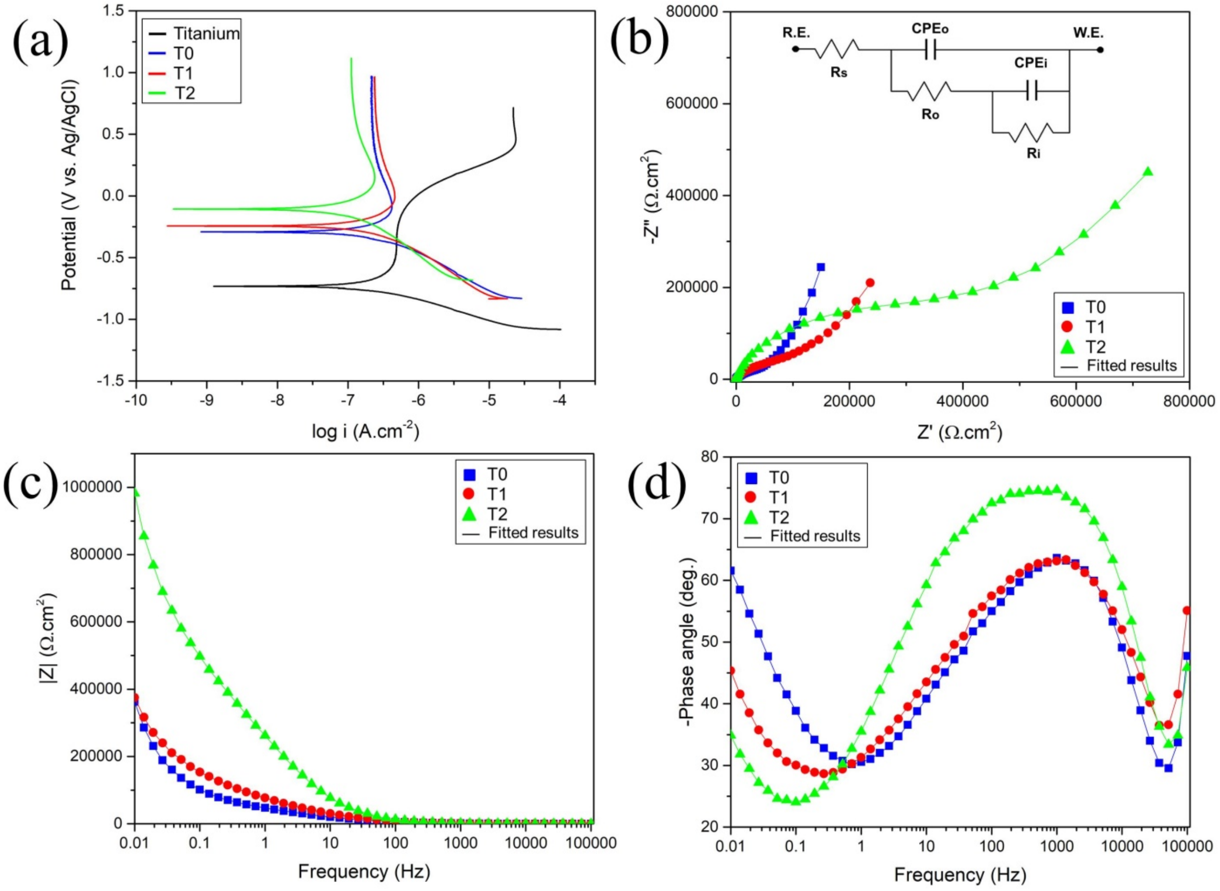

Figure 2. (a) Potentiodynamic polarization, (b) Nyquist plots along with equivalent circuit, (c) Bode modulus, and (d) Bode phase plots of the specimens.

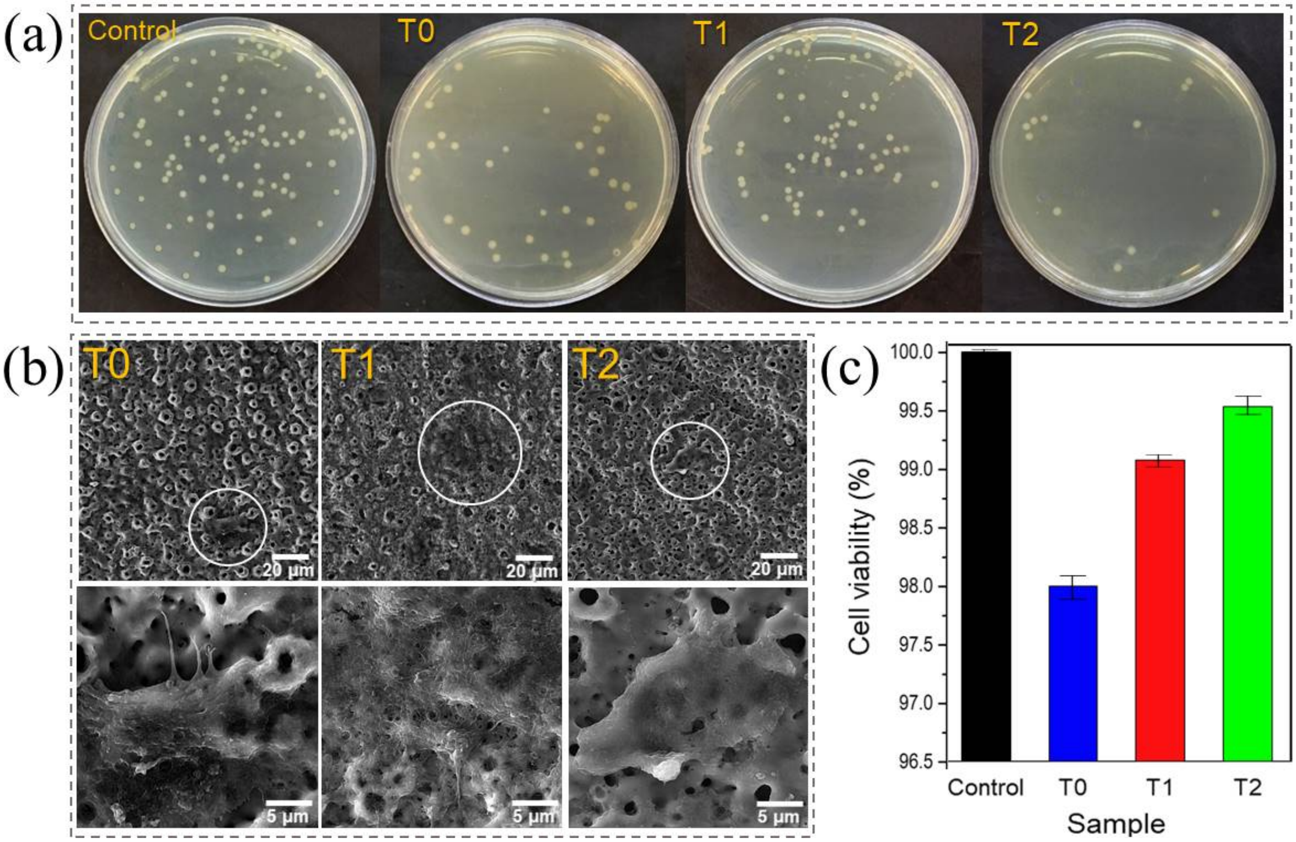

Figure 3. (a) Optical images of the cultured plates, (b) FESEM micrographs, and (c) viability of the grown MG-63 osteoblastic cells on the layers after 24 h incubation period.

Table 1. Comparative analysis of i_{corr} as a function of the elements which were incorporated into the layers on the titanium and its alloys via different surface treatment techniques.

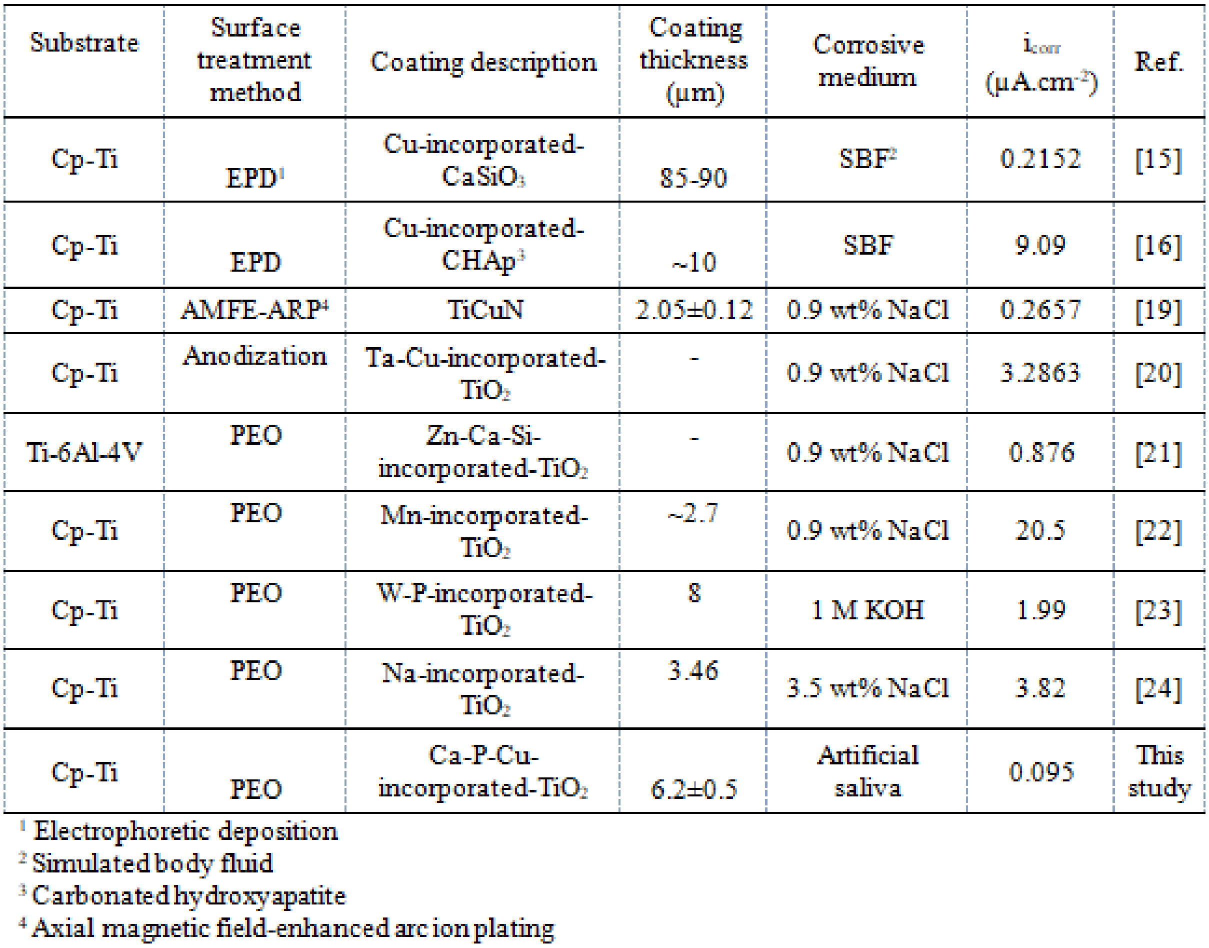

Substrate	Surface treatment method	Coating description	Coating thickness (µm)	Corrosive medium	i_{corr} (µA.cm^{-2})	Ref.
Cp-Ti	EPD[1]	Cu-incorporated-$CaSiO_3$	85-90	SBF[2]	0.2152	[15]
Cp-Ti	EPD	Cu-incorporated-CHAp[3]	~10	SBF	9.09	[16]
Cp-Ti	AMFE-ARP[4]	TiCuN	2.05±0.12	0.9 wt% NaCl	0.2657	[19]
Cp-Ti	Anodization	Ta-Cu-incorporated-TiO_2	-	0.9 wt% NaCl	3.2863	[20]
Ti-6Al-4V	PEO	Zn-Ca-Si-incorporated-TiO_2	-	0.9 wt% NaCl	0.876	[21]
Cp-Ti	PEO	Mn-incorporated-TiO_2	~2.7	0.9 wt% NaCl	20.5	[22]
Cp-Ti	PEO	W-P-incorporated-TiO_2	8	1 M KOH	1.99	[23]
Cp-Ti	PEO	Na-incorporated-TiO_2	3.46	3.5 wt% NaCl	3.82	[24]
Cp-Ti	PEO	Ca-P-Cu-incorporated-TiO_2	6.2±0.5	Artificial saliva	0.095	This study

[1] Electrophoretic deposition

[2] Simulated body fluid

[3] Carbonated hydroxyapatite

[4] Axial magnetic field-enhanced arc ion plating

Table 2. Parameters determined by fitting the EIS plots.

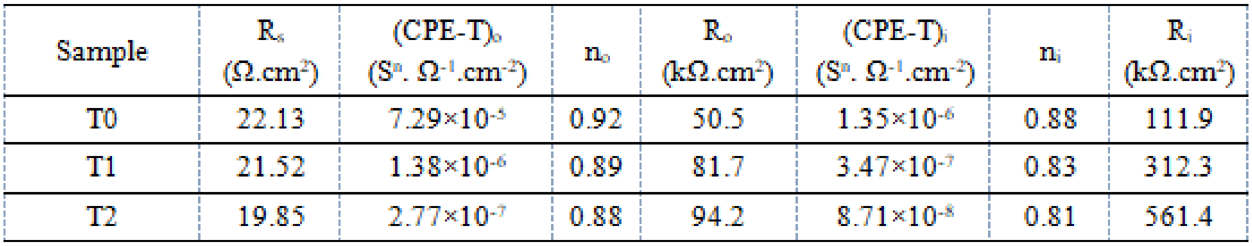

Sample	R_s (Ω.cm^2)	$(CPE\text{-}T)_o$ (S^n. Ω^{-1}.cm^{-2})	n_o	R_o (kΩ.cm^2)	$(CPE\text{-}T)_i$ (S^n. Ω^{-1}.cm^{-2})	n_i	R_i (kΩ.cm^2)
T0	22.13	7.29×10^{-5}	0.92	50.5	1.35×10^{-6}	0.88	111.9
T1	21.52	1.38×10^{-6}	0.89	81.7	3.47×10^{-7}	0.83	312.3
T2	19.85	2.77×10^{-7}	0.88	94.2	8.71×10^{-8}	0.81	561.4